







## Article

# Design and Synthesis of Multi-Functional Ligands through Hantzsch Reaction: Targeting Ca<sup>2+</sup> Channels, Activating Nrf2 and Possessing Cathepsin S Inhibitory, and Antioxidant Properties

Irene Pachón-Angona <sup>1,2,†</sup>, Paul J. Bernard <sup>1,‡</sup>, Alexey Simakov <sup>3,‡</sup> , Maciej Maj <sup>4</sup>, Krzysztof Jozwiak <sup>4</sup> , Anna Novotna <sup>5</sup>, Carina Lemke <sup>5</sup>, Michael Gütschow <sup>5</sup> , Helene Martin <sup>3</sup> , María-Jesús Oset-Gasque <sup>2,6</sup> , José-Marco Contelles <sup>7,8,\*</sup> and Lhassane Ismaili <sup>1,\*</sup> 

- <sup>1</sup> Université de Franche-Comté, UMR INSERM 1322 LINC, F-25000 Besançon, France; pachon.angona.irene@gmail.com (I.P.-A.); paul.bernard@univ-fcomte.fr (P.J.B.)
- <sup>2</sup> Department of Biochemistry and Molecular Biology, Faculty of Pharmacy, Complutense University of Madrid, Plaza Ramón y Cajal s/n, Ciudad Universitaria, 28040 Madrid, Spain; mjoset@ucm.es
- <sup>3</sup> Université de Franche-Comté, EFS, INSERM, UMR RIGHT, F-25000 Besançon, France; aleksei.simakov@univ-fcomte.fr (A.S.); helene.martin@univ-fcomte.fr (H.M.)
- <sup>4</sup> Department of Biopharmacy, Medical University of Lublin, ul. W. Chodzki 4a, 20-093 Lublin, Poland; maciej.maj@umlub.pl (M.M.); krzysztof.jozwiak@umlub.pl (K.J.)
- <sup>5</sup> Pharmaceutical Institut, An der Immenburg 4, D-53121 Bonn, Germany; novo.anna21@gmail.com (A.N.); wirtzcarina01@gmail.com (C.L.); guetschow@uni-bonn.de (M.G.)
- <sup>6</sup> Instituto Universitario de Investigación en Neuroquímica, Complutense University of Madrid, Ciudad Universitaria, 28040 Madrid, Spain
- <sup>7</sup> Laboratory of Medicinal Chemistry (IQOG, CSIC) C/Juan de la Cierva 3, 28006 Madrid, Spain
- <sup>8</sup> Center for Biomedical Network Research on Rare Diseases (CIBERER), CIBER, ISCIII, 28006 Madrid, Spain
- \* Correspondence: iqoc21@iqog.csic.es (J.-M.C.); lhassane.ismaili@univ-fcomte.fr (L.I.)
- † Current address: ETH Zurich, Institute of Pharmaceutical Sciences, Chrissula Chatzidis, HCI H 413, Vladimir-Prelog-Weg 4, CH-8093 Zurich, Switzerland.
- ‡ These authors contributed equally to this work.



**Citation:** Pachón-Angona, I.; Bernard, P.J.; Simakov, A.; Maj, M.; Jozwiak, K.; Novotna, A.; Lemke, C.; Gütschow, M.; Martin, H.; Oset-Gasque, M.-J.; et al. Design and Synthesis of Multi-Functional Ligands through Hantzsch Reaction: Targeting Ca<sup>2+</sup> Channels, Activating Nrf2 and Possessing Cathepsin S Inhibitory, and Antioxidant Properties. *Pharmaceutics* **2024**, *16*, 121. <https://doi.org/10.3390/pharmaceutics16010121>

Academic Editors: Pedro Ramos-Cabrer, Silvia Chaves and M. Amelia Santos

Received: 1 December 2023

Revised: 12 January 2024

Accepted: 13 January 2024

Published: 17 January 2024



**Copyright:** © 2024 by the authors. Licensee MDPI, Basel, Switzerland. This article is an open access article distributed under the terms and conditions of the Creative Commons Attribution (CC BY) license (<https://creativecommons.org/licenses/by/4.0/>).

**Abstract:** This work relates to the design and synthesis of a series of novel multi-target directed ligands (MTDLs), i.e., compounds **4a–l**, via a convenient one-pot three-component Hantzsch reaction. This approach targeted calcium channel antagonism, antioxidant capacity, cathepsin S inhibition, and interference with Nrf2 transcriptional activation. Of these MTDLs, **4i** emerged as a promising compound, demonstrating robust antioxidant activity, the ability to activate Nrf2-ARE pathways, as well as calcium channel blockade and cathepsin S inhibition. Dihydropyridine **4i** represents the first example of an MTDL that combines these biological activities.

**Keywords:** calcium channel inhibitors; proteases inhibitors; antioxidant response element; ORAC; Alzheimer’s disease

## 1. Introduction

Alzheimer’s disease (AD) is a complex neurodegenerative disease of the central nervous system, characterized by symptoms like memory loss, cognitive impairment and behavioural changes. It primarily affects the elderly population [1]. The number of Alzheimer’s patients is expected to reach 115 million by 2050, with significant social and economic consequences [2]. Despite its substantial impact, effective pharmaceutical solution for the disease remain limited to date [3]. Existing treatments offer only temporary relief of symptoms, and innovative monoclonal antibodies do not provide a definitive cure either.

AD possesses a multifactorial pathogenesis characterized by the accumulation of amyloid beta peptide (A $\beta$ ) and the formation of neurofibrillary tangles composed of

hyperphosphorylated tau protein [4]. These pathological structures lead to the gradual loss of cholinergic neurons and low levels of acetylcholine, resulting in memory loss and cognitive dysfunction [5].

Elevated intracellular calcium levels play a central role in AD progression. Calcium entry through L-type  $\text{Ca}^{2+}$  channels disrupts mitochondria and leads to cell death. High calcium levels also promote the formation of  $\text{A}\beta$  [6,7] and tau pathology [8]. This complex interplay between calcium,  $\text{A}\beta$ , and tau protein highlights the etiology of AD, and strategies that disrupt this cycle, such as voltage-gated calcium channel (VGCC) blockers, hold promise as a potential therapy.

Cathepsin S (Cat S), a lysosomal cysteine protease enzyme, plays a critical role in protein and antigen degradation within lysosomes. Cat S overexpression is observed in individuals with Down syndrome (DS), who also show  $\text{A}\beta$  pathology in hippocampal and neocortical neurons in the temporal lobe [9,10], and is associated with AD [9] as it facilitates tau aggregation in vitro [11]. Hence, selective cathepsin S inhibitors are emerging as potential therapeutics for the treatment of these neurodegenerative diseases [10].

Oxidative stress (OS) is another critical factor in the AD pathogenesis, resulting from a combination of events, including mitochondrial dysfunction, biometal imbalance, neuroinflammation, and hydrogen peroxide production [12–15]. OS is the result of an imbalance between several endogenous antioxidant/pro-oxidant mechanisms, resulting in the oxidant species overproduction. The Keap1-Nrf2-ARE signaling pathway regulates antioxidant defenses and plays a crucial role in the OS and detoxification processes when activated. This pathway involves several key components: Keap1 (Kelch-like ECH-associated protein 1), Nrf2 (nuclear factor (erythroid-derived 2)-like 2), and ARE (antioxidant response element) [16].

In light of the above, the development of multitarget directed ligands (MTDLs), i.e., single small molecules that modulate multiple biological targets responsible for AD pathogenesis, has been the focus of intense research [17–21].

Our research focuses on multicomponent reactions (MCRs), not only for their ability to generate high structural diversity but also as environmentally friendly synthesis tools [22–24]. Continuing our contributions in this field, we present the design, synthesis through Hantzsch-MCR, and the biological assessment of a novel family of MTDLs (4a–l). These compounds have been designed (see Figure 1) based on the combination of dihydropyridines (DHPs), which exhibit an inherent calcium channel modulation activity [25,26], and propargyl amide residues as electrophilic substructures.

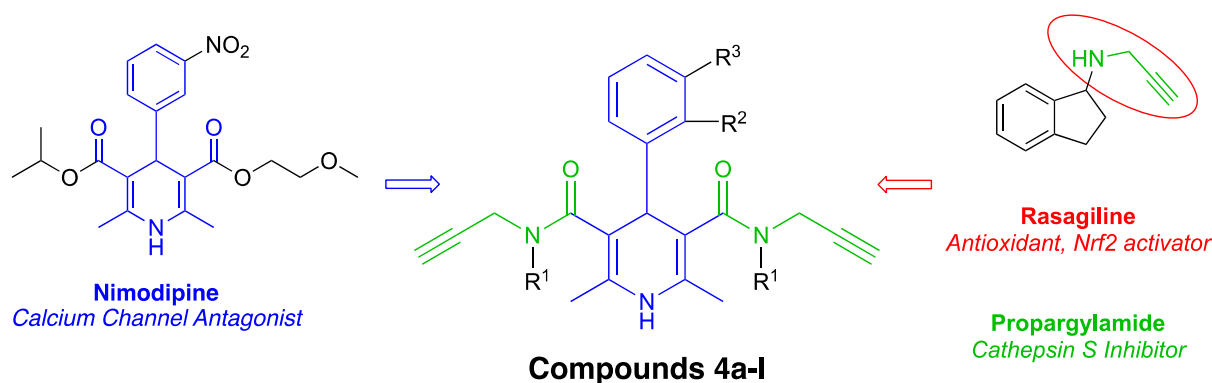


**Figure 1.** Design of compounds 4a–l.

DHPs play a crucial role in medicinal chemistry, serving as the fundamental building blocks for widely used calcium channel antagonists such as nifedipine, nivaldipine, and others. Importantly, elevated cytosolic calcium levels, implicated in the pathogenesis of AD, contribute to the generation of  $\text{A}\beta$  peptides through calcium-mediated  $\beta$ -secretase activity [6,7,27–29]. They also regulate glycogen synthase kinase, leading to tau hyperphosphorylation and increased neurofibrillary tangle (NFT) formation [8]. Consequently,

calcium channel antagonists, including DHPs, may exert a neuroprotective influence by inhibiting the development of A $\beta$  peptides and NFTs, which are key features of AD [30].

Propargylamines are known as antioxidant residues capable of effectively scavenging reactive oxygen species (ROS) and reactive nitrogen species (RNS) [31–33]. The propargyl moiety in trade drugs, such as selegiline and rasagiline, is responsible for the nuclear translocation of Nrf2 activity and is able to enhance its binding to the ARE [34]. Additionally, propargyl amides have been studied as irreversible inhibitors of cysteine proteases such as Cap S [35]. Thus, including this feature in the structure of these hybrid compounds could improve their pharmacological profile, providing an additional neuroprotective effect [36].

## 2. Materials and Methods

Melting points ( $^{\circ}$ C) were determined using a Kofler hot bench and are reported without correction.

The reaction progress was monitored using thin-layer chromatography (TLC, Silica gel 60 F254, 0.25 mm thickness; Merck, Darmstadt, Germany). NMR spectra were recorded on a Bruker Avance DRX 400 instrument in either CDCl<sub>3</sub> containing tetramethylsilane or DMSO-*d*<sub>6</sub> as solvents. <sup>1</sup>H and <sup>13</sup>C chemical shifts are reported in part per million (ppm) using tetramethylsilane (0.00 ppm) or residual solvent (DMSO-*d*<sub>6</sub>, 2.50/39.52 ppm) as an internal reference standard. BRUKER micro TOF-Q mass spectrometers were used to acquire the mass spectra at UCA Clermont Ferrand, France. The elemental analyses were carried out on a Carlo Erba EA 1108 analyser

**General procedure for the synthesis of acetoacetamides (2a–b).** Acetoacetamides (2a–b) were synthesized as described by Clemens et al. [37] A solution of 2,2,6-trimethyl-4*H*-1,3-dioxin-4-one (1 equiv.) and the corresponding propargylic amine (1 equiv.) was refluxed in xylene (10 mmol/mL) over 150 min. The reaction was quenched by adding CH<sub>2</sub>Cl<sub>2</sub>, and solvents were removed in vacuo. The residue was purified by flash column to afford final acetoacetamides with 25–72% of yields.

**3-Oxo-*N*-(prop-2-yn-1-yl)butanamide (2a).** The crude material was synthesized following the general procedure from propargylamine **1a** (1 equiv., 50 mmol, 6.67 mL) and 2,2,6-trimethyl-4*H*-1,3-dioxin-4-one (1 equiv., 50 mmol, 3.20 mL) in xylene (5 mL) to afford 3.50 g of the desired compound (25%). <sup>1</sup>H NMR (400 MHz, CDCl<sub>3</sub>)  $\delta$  7.33 (s, 1H), 4.06 (dd, *J* = 5.2, 2.5 Hz, 2H), 3.44 (s, 2H), 2.26 (s, 3H), 2.22 (t, *J* = 2.4 Hz, 1H), 1.24 (s, 1H). <sup>13</sup>C NMR (101 MHz, CDCl<sub>3</sub>)  $\delta$  204.51, 165.40, 79.30, 71.71, 49.16, 31.20, 29.20.

***N*-Methyl-3-oxo-*N*-(prop-2-yn-1-yl)butanamide (2b).** The crude material was synthesized following the general procedure from *N*-methylpropargylamine **1b** (1 equiv., 22.58 mmol, 1.90 mL) and 2,2,6-trimethyl-4*H*-1,3-dioxin-4-one (1 equiv., 22.85 mmol, 3 mL) in xylene (6 mL) to afford 2.5 g of the desired compound (72%). <sup>1</sup>H NMR (400 MHz, CDCl<sub>3</sub>)  $\delta$  4.17 (t, *J* = 2.4 Hz, 1.30H) and 3.97 (t, *J* = 2.1 Hz, 0.70H), 3.55 (d, *J* = 1.9 Hz, 0.60H) and 3.49 (d, *J* = 1.9 Hz, 1.40H), 2.99 (d, *J* = 2.2 Hz, 1.27H) and 2.95 (d, *J* = 2.9 Hz, 1.73H), 2.31 (t, *J* = 2.5 Hz, 0.25H) and 1.90 (t, *J* = 2.3 Hz, 0.75H), 2.24–2.16 (m, 2H). <sup>13</sup>C NMR (101 MHz, CDCl<sub>3</sub>)  $\delta$  202.28 and 202.00, 175.53 and 166.49, 78.18, 73.35 and 72.21, 49.92 and 49.80, 40.01, and 36.27, 34.98 and 33.47, 30.33 and 30.21.

**General procedure for the synthesis of Hantzsch derivatives (4a–l).** Commercial aldehyde (1 equiv.) and corresponding acetoacetamide (2 equiv.) were dissolved in a minimum volume of EtOH. Subsequently, an equivalent volume of water was gradually added drop by drop, accompanied by ultrasonic treatment of the crude mixture. Ammonium carbonate (1.2 equiv.) was finally added, and the reaction was stirred and heated overnight. The desired compounds (**4a–l**) are obtained by filtration, recrystallization, or purification by flash column chromatography, affording yields from 5 to 55%.

**2,6-Dimethyl-4-phenyl-*N*3,*N*5-bis(prop-2-yn-1-yl)-1,4-dihydropyridine-3,5-dicarboxamide (4a).** This compound was prepared according to the general procedure from benzaldehyde (1 equiv., 1.79 mmol, 0.18 mL), 3-oxo-*N*-(prop-2-yn-1-yl)butanamide **2a** (2 equiv., 3.59 mmol, 500 mg), and ammonium carbonate (1.2 equiv., 2.15 mmol, 207 mg) at 35  $^{\circ}$ C over 14 h. The precipitated **4a** was filtered, triturated in a mixture

of pentane and diethyl ether (1:1 *v/v*), and then filtered again, ultimately yielding 48.20 mg (15%) as a beige powder.  $^1\text{H}$  NMR (400 MHz, DMSO- $d_6$ )  $\delta$  7.96 (s, 1H), 7.72 (t,  $J = 5.5$  Hz, 2H), 7.21–7.05 (m, 5H), 4.75 (s, 1H), 3.85 (qdd,  $J = 17.4, 5.5, 2.4$  Hz, 4H), 3.04 (t,  $J = 2.4$  Hz, 2H), 2.08 (s, 6H).  $^{13}\text{C}$  NMR (101 MHz, DMSO- $d_6$ )  $\delta$  168.05, 146.63, 138.86, 128.02, 126.91, 125.86, 104.04, 81.80, 72.44, 27.86, 17.35. Anal. Calcd. for  $\text{C}_{21}\text{H}_{20}\text{N}_3\text{O}_2$ : C, 72.60; H, 6.09; N, 12.10; found: C, 70.86; H, 6.19; N, 12.23.

**2,6-Dimethyl-4-(3-nitrophenyl)-N3,N5-bis(prop-2-yn-1-yl)-1,4-dihydropyridine-3,5-dicarboxamide (4b).** Compound 4b was prepared according to the general procedure starting from 2-nitrobenzaldehyde (1 equiv., 1.79 mmol, 270 mg), 3-oxo-*N*-(prop-2-yn-1-yl)butanamide 2a (2 equiv., 3.59 mmol, 500 mg), and ammonium carbonate (2.3 equiv., 4.32 mmol, 414 mg). After 15 h,  $\text{H}_2\text{O}$  was poured into the reaction crude, extracted 5 times with  $\text{CH}_2\text{Cl}_2$ , and then dried over  $\text{Na}_2\text{SO}_4$ . The substance was filtered and subjected to purification through flash column chromatography using  $\text{CH}_2\text{Cl}_2/\text{MeOH}$  (95/5) with 1%  $\text{NH}_3$  as the eluent. This process resulted in the final yield of 121 mg (8.75%) of 4b in the form of bright orange crystals.  $^1\text{H}$  NMR (400 MHz, DMSO- $d_6$ )  $\delta$  8.16 (s, 1H), 7.70–7.57 (m, 4H), 7.51 (dd,  $J = 7.9, 1.4$  Hz, 1H), 7.38–7.29 (m, 1H), 5.25 (s, 1H), 3.77 (dddd,  $J = 51.5, 17.4, 5.4, 2.5$  Hz, 4H), 3.01 (t,  $J = 2.5$  Hz, 2H), 2.06 (s, 6H).  $^{13}\text{C}$  NMR (101 MHz, DMSO- $d_6$ )  $\delta$  167.43, 147.08, 141.59, 139.14, 133.44, 130.96, 127.27, 123.29, 104.08, 81.27, 72.70, 36.06, 27.96, 17.39. Anal. Calcd. for  $\text{C}_{21}\text{H}_{20}\text{N}_4\text{O}_4$ : C, 64.28; H, 5.14; N, 14.28; found: C, 63.11; H, 5.19; N, 14.39.

**2,6-Dimethyl-4-(2-nitrophenyl)-N3,N5-bis(prop-2-yn-1-yl)-1,4-dihydropyridine-3,5-dicarboxamide (4c).** This compound was prepared according to the general procedure from 3-nitrobenzaldehyde (1 equiv., 1.79 mmol, 272 mg), 3-oxo-*N*-(prop-2-yn-1-yl)butanamide 2a (2 equiv., 3.59 mmol, 500 mg), and ammonium carbonate (1.2 equiv., 2.16 mmol, 207 mg) at 50 °C over 15 h. Precipitated 4c was filtered, washed in diethyl ether, and filtered again to finally afford 275.5 mg (39%) as a bright yellow powder.  $^1\text{H}$  NMR (400 MHz, DMSO- $d_6$ )  $\delta$  8.13 (s, 1H), 8.01–7.93 (m, 2H), 7.89 (t,  $J = 5.6$  Hz, 2H), 7.59 (d,  $J = 7.7$  Hz, 1H), 7.50 (td,  $J = 7.7, 1.2$  Hz, 1H), 4.92 (s, 1H), 3.89–3.74 (m, 4H), 2.98 (t,  $J = 2.4$  Hz, 2H), 2.08 (s, 6H).  $^{13}\text{C}$  NMR (101 MHz, DMSO- $d_6$ )  $\delta$  167.67, 148.96, 147.71, 139.11, 133.94, 129.45, 121.68, 120.99, 103.62, 81.69, 72.28, 40.52, 27.88, 17.38. Anal. Calcd. for  $\text{C}_{21}\text{H}_{20}\text{N}_4\text{O}_4$ : C, 64.28; H, 5.14; N, 14.28; found: C, 63.39; H, 5.11; N, 14.39.

**4-(2,1,3-Benzoxadiazol-4-yl)-2,6-dimethyl-N3,N5-bis(prop-2-yn-1-yl)-1,4-dihydropyridine-3,5-dicarboxamide (4d).** Compound 4d was prepared according to the general procedure from 2,1,3-benzoxadiazole-4-benzaldehyde (1 equiv., 0.72 mmol, 107 mg), 3-oxo-*N*-(prop-2-yn-1-yl)butanamide 2a (2 equiv., 1.47 mmol, 200 mg) and ammonium carbonate (1.2 equiv., 0.86 mmol, 83 mg) at 50 °C over 15 h. Then, the mixture was cooled to room temperature, and precipitated 4d was filtered and resuspended in toluene. The solvent was removed under reduced pressure, and the residue was washed with diethyl ether and filtered again to finally afford 141.5 mg (51%) of 4d as a dark yellowish powder.  $^1\text{H}$  NMR (400 MHz, DMSO- $d_6$ )  $\delta$  8.15 (s, 1H), 7.87–7.73 (m, 3H), 7.46 (dd,  $J = 8.8, 6.8$  Hz, 1H), 7.13 (d,  $J = 6.6$  Hz, 1H), 5.23 (s, 1H), 3.90–3.67 (m, 4H), 2.96 (s, 2H), 2.03 (s, 6H).  $^{13}\text{C}$  NMR (101 MHz, DMSO- $d_6$ )  $\delta$  167.78, 149.51, 148.05, 138.95, 134.57, 132.92, 127.93, 113.41, 102.32, 81.64, 72.29, 27.88, 17.27. Anal. Calcd. for  $\text{C}_{21}\text{H}_{19}\text{N}_5\text{O}_5$ : C, 64.77; H, 4.92; N, 17.98; found: C, 62.89; H, 4.88; N, 18.08.

**4-(2-Chlorophenyl)-2,6-dimethyl-N3,N5-bis(prop-2-yn-1-yl)-1,4-dihydropyridine-3,5-dicarboxamide (4e).** This compound was prepared according to the general procedure starting from 2-chlorobenzaldehyde (1 equiv., 1.80 mmol, 0.20 mL), 3-oxo-*N*-(prop-2-yn-1-yl)butanamide 2a (2 equiv., 3.59 mmol, 500 mg), and ammonium carbonate (1.2 equiv., 2.16 mmol, 207 mg) at 45 °C over 15 h. Then, it was cooled to room temperature and extracted with  $\text{CH}_2\text{Cl}_2$  three times. Organic layers were combined, dried over  $\text{Na}_2\text{SO}_4$ , and evaporated. The residue was washed with diethyl ether and filtered to afford 129 mg (56%) of 4e as a white powder.  $^1\text{H}$  NMR (400 MHz, DMSO- $d_6$ )  $\delta$  7.96 (s, 1H), 7.72 (s, 2H), 7.28 (d,  $J = 7.3$  Hz, 1H), 7.24–7.19 (m, 2H), 7.10 (t,  $J = 7.1$  Hz, 1H), 5.10 (s, 1H), 3.82 (d,  $J = 2.7$  Hz, 4H), 3.04 (s, 2H), 2.01 (s, 6H).  $^{13}\text{C}$  NMR (101 MHz, DMSO- $d_6$ )  $\delta$  167.98, 144.83,

137.89, 130.79, 130.16, 128.73, 127.61, 127.48, 104.47, 81.49, 72.69, 40.20, 27.89, 16.97. Anal. Calcd. for  $C_{21}H_{20}ClN_3O_2$ : C, 66.05; H, 5.28; N, 11.00; found: C, 64.86; H, 5.31; N, 10.91.

**4-(2-Methoxyphenyl)-2,6-dimethyl-N3,N5-bis(prop-2-yn-1-yl)-1,4-dihydropyridine-3,5-dicarboxamide (4f).** Compound **4f** was prepared according to the general procedure starting from 2-methoxybenzaldehyde (1 equiv., 0.72 mmol, 0.087 mL), 3-oxo-N-(prop-2-yn-1-yl)butanamide **2a** (2 equiv., 1.44 mmol, 200 mg), and ammonium carbonate (1.7 equiv., 0.86 mmol, 119 mg) at 50 °C over 15 h. Then, it was cooled to room temperature, and water was poured into the mixture. Precipitated **4f** was filtered and washed with diethyl ether to afford 78.7 mg (30%) as a light yellowish solid.  $^1H$  NMR (400 MHz, DMSO- $d_6$ )  $\delta$  8.05 (s, 1H), 7.42 (s, 2H), 7.20–7.05 (m,  $J$  = 16.1, 7.6 Hz, 3H), 6.86 (t,  $J$  = 8.2 Hz, 2H), 4.92 (s, 1H), 3.92–3.74 (m, 7H), 3.07 (s, 2H), 2.12 (s, 6H).  $^{13}C$  NMR (101 MHz, DMSO- $d_6$ )  $\delta$  167.47, 153.60, 139.92, 135.88, 129.43, 127.43, 121.29, 110.45, 104.13, 81.50, 72.80, 55.56, 32.69, 28.11, 17.55. HRMS ESI-TOF  $[M]^+$   $m/z$  calcd. for  $C_{22}H_{23}N_3O_3$ : 377,1724, found: 377,1739.

**4-(2-Bromophenyl)-2,6-dimethyl-N3,N5-bis(prop-2-yn-1-yl)-1,4-dihydropyridine-3,5-dicarboxamide (4g).** This compound was prepared according to the general procedure starting from 2-bromobenzaldehyde (1 equiv., 1.08 mmol, 0.126 mL), 3-oxo-N-(prop-2-yn-1-yl)butanamide **2a** (2 equiv., 2.16 mmol, 300 mg), and ammonium carbonate (1.2 equiv., 1.29 mmol, 124 mg) at 45 °C over 15 h. Precipitated **4g** was filtered and washed with diethyl ether over 1 h to afford 154 mg (34%) as a white solid.  $^1H$  NMR (400 MHz, DMSO- $d_6$ )  $\delta$  7.96 (s, 1H), 7.71 (t,  $J$  = 5.1 Hz, 2H), 7.38 (d,  $J$  = 7.9 Hz, 1H), 7.32–7.19 (m, 2H), 7.09–6.96 (m, 1H), 5.07 (s, 1H), 3.95–3.75 (m, 4H), 3.05 (s, 2H), 2.00 (s, 6H).  $^{13}C$  NMR (101 MHz, DMSO- $d_6$ )  $\delta$  167.98, 146.90, 137.54, 132.00, 131.03, 128.18, 128.00, 120.49, 104.90, 81.47, 72.78, 41.59, 27.89, 16.91. Anal. Calcd. for  $C_{22}H_{23}BrN_3O_3$ : C, 59.17; H, 4.73; N, 9.86; found: C, 58.79; H, 4.80; N, 9.88.

**4-(3-Bromophenyl)-2,6-dimethyl-N3,N5-bis(prop-2-yn-1-yl)-1,4-dihydropyridine-3,5-dicarboxamide (4h).** Compound **4h** was prepared according to the general procedure starting from 2-bromobenzaldehyde (1 equiv., 1.08 mmol, 0.126 mL), 3-oxo-N-(prop-2-yn-1-yl)butanamide **2a** (2 equiv., 2.157 mmol, 300 mg), and ammonium carbonate (1.2 equiv., 1.29 mmol, 124 mg) at 45 °C over 15 h. Precipitated **4h** was filtered and washed with diethyl ether over 1 h to afford 56.8 mg (12%) as a white solid.  $^1H$  NMR (400 MHz, DMSO- $d_6$ )  $\delta$  8.03 (s, 1H), 7.80 (t,  $J$  = 5.1 Hz, 2H), 7.33–7.25 (m, 2H), 7.20–7.07 (m, 2H), 4.77 (s, 1H), 3.84 (qd,  $J$  = 17.3, 3.1 Hz, 4H), 3.02 (s, 2H), 2.07 (s, 6H).  $^{13}C$  NMR (101 MHz, DMSO- $d_6$ )  $\delta$  167.82, 149.33, 139.00, 130.21, 129.64, 128.76, 126.03, 121.56, 103.68, 81.74, 72.42, 40.34, 27.87, 17.36. Anal. Calcd. for  $C_{22}H_{23}BrN_3O_3$ : C, 59.17; H, 4.73; N, 9.86; found: C, 57.88; H, 4.69; N, 9.78.

**4-(2-Chlorophenyl)-N2,N3,5,6-tetramethyl-N3,N5-bis(prop-2-yn-1-yl)-1,4-dihydropyridine-3,5-dicarboxamide (4i).** This compound was prepared according to the general procedure from 2-chlorobenzaldehyde (1 equiv., 1.09 mmol, 0.126 mL), *N*-methyl-3-oxo-N-(prop-2-yn-1-yl)butanamide **2b** (3 equiv., 3.27 mmol, 500 mg), and ammonium carbonate (1.2 equiv., 1.96 mmol, 188 mg) at 55 °C over 19 h.  $CH_2Cl_2$  was added to the mixture. The organic layer was washed with water and brine, then dried over  $Na_2SO_4$  and evaporated to finally be purified by flash column chromatography using 25/75 hexane/EtOAc + 1%  $Et_3N$  as eluent. **4i** was washed with pentane:diethyl ether 1:1 *v/v* and filtered to finally afford 95 mg (12%) as a light beige solid.  $^1H$  NMR (400 MHz, DMSO- $d_6$ )  $\delta$  7.78 (s, 1H), 7.38 (bs, 1H), 7.29–7.19 (m, 2H), 7.16–7.07 (m, 1H), 4.93 (s, 1H), 4.00 (t,  $J$  = 19.3 Hz, 4H), 3.13 (s, 2H), 2.78 (s, 6H), 1.74 (s, 6H).  $^{13}C$  NMR (101 MHz, DMSO- $d_6$ )  $\delta$  169.92, 133.23, 131.20, 127.80, 127.32, 79.15, 74.33, 15.94. Anal. Calcd. for  $C_{23}H_{24}ClN_3O_2$ : C, 67.39; H, 5.90; N, 10.25; found: C, 66.12; H, 5.98; N, 10.30.

**4-(2,3-Dichlorophenyl)-N2,N3,5,6-tetramethyl-N3,N5-bis(prop-2-yn-1-yl)-1,4-dihydropyridine-3,5-dicarboxamide (4j).** Compound **4j** was prepared according to the general procedure starting from 2,3-dichlorobenzaldehyde (1 equiv., 1.14 mmol, 200 mg), *N*-methyl-3-oxo-N-(prop-2-yn-1-yl)butanamide **2b** (2 equiv., 2.29 mmol, 350 mg), and ammonium carbonate (1.2 equiv., 1.37 mmol, 140 mg) at 45 °C over 19 h. Diethyl ether was added to the reaction crude. The organic layer was washed with water and brine, then dried over  $Na_2SO_4$ , and evaporated under reduced pressure to finally be purified by flash



column chromatography using 94/6 CH<sub>2</sub>Cl<sub>2</sub>/MeOH + 1% NH<sub>3</sub> as eluent. 4j was washed with pentane:diethyl ether 1:1 *v/v* and filtered to finally afford 21.3 mg (7%) as a light yellow powder. <sup>1</sup>H NMR (400 MHz, DMSO-*d*<sub>6</sub>) δ 7.88 (s, 1H), 7.44–7.34 (m, 2H), 7.30 (d, *J* = 6.7 Hz, 1H), 4.99 (s, 1H), 4.05 (dd, *J* = 30.9, 17.2 Hz, 4H), 3.13 (s, 2H), 2.81 (s, 6H), 1.74 (s, 6H). <sup>13</sup>C NMR (101 MHz, DMSO-*d*<sub>6</sub>) δ 169.72, 133.66, 129.72, 128.33, 128.11, 101.86, 74.33, 15.95, 13.90. HRMS ESI-TOF [M]<sup>+</sup> *m/z* calcd. for C<sub>23</sub>H<sub>23</sub>Cl<sub>2</sub>N<sub>3</sub>O<sub>2</sub>: 443,1149, found: 443,1167.

**4-(2-Methoxyphenyl)-N2,N3,5,6-tetramethyl-N3,N5-bis(prop-2-yn-1-yl)-1,4-dihydropyridine-3,5-dicarboxamide (4k).** This compound was prepared according to the general procedure starting from 2-methoxybenzaldehyde (1 equiv., 1.63 mmol, 0.197 mL), *N*-methyl-3-oxo-*N*-(prop-2-yn-1-yl)butanamide **2b** (2 equiv., 3.27 mmol, 500 mg), and ammonium carbonate (1.2 equiv., 1.96 mmol, 188 mg) at 40 °C over 15 h. Diethyl ether was added to the reaction crude. The organic layer was washed with water and brine, then dried over Na<sub>2</sub>SO<sub>4</sub> and reduced under pressure conditions to finally be purified by flash column chromatography using 96/4 CH<sub>2</sub>Cl<sub>2</sub>/MeOH + 1% NH<sub>3</sub> as eluent. 4k was washed with pentane:diethyl ether 1:1 *v/v* over 1 h and filtered to finally afford 45.6 mg (7%) as a light beige powder. <sup>1</sup>H NMR (400 MHz, DMSO-*d*<sub>6</sub>) δ 7.60 (s, 1H), 7.18–7.04 (m, 2H), 6.83 (dd, *J* = 16.3, 7.9 Hz, 2H), 4.78 (s, 1H), 4.01 (t, *J* = 20.9 Hz, 4H), 3.62 (s, 3H), 3.15 (s, 2H), 2.76 (s, 6H), 1.73 (s, 6H). <sup>13</sup>C NMR (101 MHz, DMSO-*d*<sub>6</sub>) δ 170.58, 129.27, 127.22, 120.25, 110.47, 102.15, 94.29, 79.49, 74.06, 64.90, 55.20, 46.98, 34.46, 15.93. HRMS ESI-TOF [M]<sup>+</sup> *m/z* calcd. for C<sub>24</sub>H<sub>27</sub>N<sub>3</sub>O<sub>3</sub>: 405,2042, found: 405,2052.

**4-(3-Methoxyphenyl)-N2,N3,5,6-tetramethyl-N3,N5-bis(prop-2-yn-1-yl)-1,4-dihydropyridine-3,5-dicarboxamide (4l).** Compound **4l** was prepared according to the general procedure starting from 3-methoxybenzaldehyde (1 equiv., 1.63 mmol, 0.197 mL), *N*-methyl-3-oxo-*N*-(prop-2-yn-1-yl)butanamide **2b** (2 equiv., 3.27 mmol, 500 mg), and ammonium carbonate (1.2 equiv., 1.96 mmol, 188 mg) at 45 °C over 15 h. CH<sub>2</sub>Cl<sub>2</sub> was added to the reaction mixture. The organic layer was washed with water, brine, then dried over Na<sub>2</sub>SO<sub>4</sub> and evaporated to finally be purified by flash column chromatography using 96/4 CH<sub>2</sub>Cl<sub>2</sub>/MeOH + 1% NH<sub>3</sub> as eluent. **4l** was washed with pentane:diethyl ether 1:1 *v/v* over 1 h and filtered to finally afford 56.5 mg (5%) as light beige powder. <sup>1</sup>H NMR (400 MHz, DMSO-*d*<sub>6</sub>) δ 7.66 (s, 1H), 7.12 (t, *J* = 7.6 Hz, 1H), 6.67 (dd, *J* = 24.2, 7.4 Hz, 2H), 6.55 (s, 1H), 4.44 (s, 1H), 4.00 (s, 4H), 3.67 (s, 3H), 3.14 (s, 2H), 2.72 (s, 6H), 1.73 (s, 6H). <sup>13</sup>C NMR (101 MHz, DMSO-*d*<sub>6</sub>) δ 170.48, 159.14, 146.53, 129.15, 119.76, 113.00, 111.48, 102.62, 79.26, 54.84, 44.85, 16.01. HRMS ESI-TOF [M]<sup>+</sup> *m/z* calcd. for C<sub>24</sub>H<sub>27</sub>N<sub>3</sub>O<sub>3</sub>: 405,2040, found: 405,2052.

**Calcium channel blockade.** Evaluation of the calcium channel blockade of compounds **4a–I** was performed using the FLIPR Calcium 6 indicator according to a previously established protocol [38]. Briefly, human neuroblastoma cell line SH-SY5Y seeded out on 96-well plate were treated with fluorescent calcium indicator (FLIPR Calcium 6, Molecular Devices). Cells were incubated with indicator for 2 h at 37 °C, facilitating internalization of the indicator. Subsequently, cells were exposed to nimodipine (10 μM, used as reference inhibitor), DMSO (0.1%, used as vehicle control) or our compounds of interest (10 μM) for 10 min also at 37 °C. Following that, cell fluorescence was recorded using a microplate reader (λ<sub>Ex</sub> = 485 nm; λ<sub>Em</sub> = 525 nm). Baseline fluorescence was recorded for 5 s. Afterwards, cells were stimulated by the addition of the solution of KCl and CaCl<sub>2</sub> (90 and 5 mM, respectively) in order to induce the opening of voltage-gated calcium channels. An increase in fluorescence of calcium indicator after inducing calcium flux was recorded for another 30 s. Data were collected from three independent experiments, with eight technical replicates per experiment. Fluorescence intensity values were normalized to the baseline recorded before the induction of calcium flux. The percentage of inhibition was calculated as a reduction of normalized calcium flux in comparison with the DMSO vehicle control. Outliers were detected using the Grubbs test, and any outlying values were excluded from further analysis.

**Oxygen radical absorbance capacity assay.** The evaluation of the antioxidant activity of compounds **4a–I** was carried out using the previously established ORAC-FL method [38], and detailed information is provided in the supporting information.

**Nrf2 transcriptional activation potencies.** The assessment of the Nrf2 transcriptional activation potencies of compounds **4a–l** was carried out using the previously described method [38], and detailed information is provided in the supporting information.

**Cathepsin assays.** Assays with human cathepsins B, S, L, and K were carried out as described previously [39–41]. Stock solutions of substrates and inhibitors were prepared in DMSO. The final DMSO concentration was 2%. All test compounds were investigated in duplicate at a concentration of 50  $\mu\text{M}$  to determine residual activities based on endpoints of substrate consumption after 60 min.  $K_i$  values were obtained in duplicate measurements with six different inhibitor concentrations, and 60-min-progress curves were analyzed by linear regression.  $\text{IC}_{50}$  values were obtained by non-linear regression using the equation  $v_i = v_0 / (1 + ([I]/\text{IC}_{50}))$ , where  $v_i$  is the product formation rate at different inhibitor concentrations,  $v_0$  is the uninhibited product formation rate,  $[I]$  is the inhibitor concentration, and  $\text{IC}_{50}$  is the half-maximal inhibitory concentration.  $\text{IC}_{50}$  values are transformed to  $K_i$  values using the Cheng-Prusoff equation.

Human isolated cathepsin B (Calbiochem) was assayed spectrophotometrically (Cary 50 Bio, Varian) at 405 nm and 37 °C. Assay buffer was 100 mM sodium phosphate buffer pH 6.0, 100 mM NaCl, 5 mM EDTA, 0.01% Brij 35. For activation, an enzyme stock solution was diluted with assay buffer containing 5 mM DTT and incubated for 30 min at 37 °C. The final concentration of the chromogenic substrate Z-Arg-Arg-pNA was 500  $\mu\text{M}$  ( $0.45 \times K_m$ ).

Human recombinant cathepsin S (Enzo Life Sciences) was assayed fluorometrically (FLUOstar Optima plate reader, BMG Labtech) at 25 °C with an emission wavelength of 360 nm and an absorption wavelength of 460 nm. The assay buffer was 100 mM sodium phosphate buffer pH 6.0, 100 mM NaCl, 5 mM EDTA, 0.01% Brij 35. For activation, an enzyme stock solution was diluted with assay buffer containing 5 mM DTT and incubated for 60 min at 37 °C. The final concentration of the chromogenic substrate Z-Phe-Arg-AMC was 40  $\mu\text{M}$  ( $0.74 \times K_m$ ).

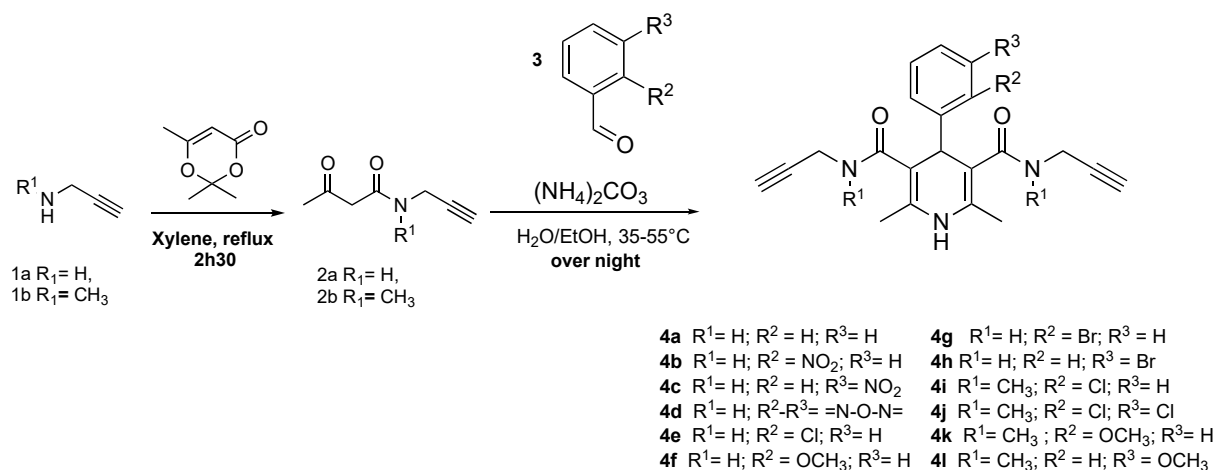
Human isolated cathepsin L (Enzo Life Sciences) was assayed spectrophotometrically (Cary 50 Bio, Varian) at 405 nm and 37 °C. The assay buffer was 100 mM sodium phosphate buffer pH 6.0, 100 mM NaCl, 5 mM EDTA, and 0.01% Brij 35. For activation, an enzyme stock solution was diluted with assay buffer containing 5 mM DTT and incubated for 30 min at 37 °C. The final concentration of the chromogenic substrate Z-Phe-Arg-pNA was 100  $\mu\text{M}$  ( $5.88 \times K_m$ ).

Human recombinant cathepsin K (Enzo Life Sciences) was assayed fluorometrically (FLUOstar Optima plate reader, BMG Labtech) with an emission wavelength of 360 nm and an absorption wavelength of 460 nm. The assay buffer was 100 mM sodium citrate pH 5.0, 100 mM NaCl, 1 mM EDTA, 0.01% CHAPS. For activation, an enzyme stock solution was diluted with assay buffer containing 5 mM DTT and incubated for 30 min at 37 °C. The final concentration of the chromogenic substrate Z-Leu-Arg-AMC was 40  $\mu\text{M}$  ( $13.33 \times K_m$ ).

### 3. Results and Discussion

#### 3.1. Synthesis

The synthesis of the new MTDL **4a–l** was carried out according to the modified Hantzsch reaction protocol reported by Tamaddon et al. [42] using acetoacetamides **2a–b**, ammonium carbonate, and aldehydes **3** in a mixture of EtOH/water (1:1 *v/v*) at 35–55 °C overnight (Scheme 1). The acetoacetamides were prepared according to the protocol described by Clemens and Hyatt [37]. The reaction started with commercially available prop-2-yn-1-amine (**1a**) or *N*-methylprop-2-yn-1-amine (**1b**) and 2,2,6-trimethyl-4*H*-1,3-dioxin-4-one in xylene at reflux to give the desired acetoacetamide and acetone. All new compounds were characterized using  $^1\text{H}$  and  $^{13}\text{C}$  NMR and HRMS or elemental analysis, and their structures are collected in the Experimental Section.



Scheme 1. Synthesis of MTDLs 4a–l.

### 3.2. Biological Evaluation

**Calcium channel blockade.** The Ca<sup>2+</sup> channel blocking capacity of compounds 4a–l and nimodipine, used as a standard at a concentration of 10 μM, was evaluated according to an established methodology [38]. As outlined in Table 1, three compounds showed no activity, while the observed percentage values for others ranged from 3 (4c) to 19 (4f), with nimodipine exhibiting 37%. The most potent compounds, in descending order, were 4f (19%), 4l (15%) and 4k (14%), representing approximately half the activity observed for nimodipine (37%). No structure–activity relationship could be established from these results.

Table 1. Biological activities of compounds 4a–l.

Compd	R <sup>1</sup>	R <sup>2</sup>	R <sup>3</sup>	Calcium Channel Blockade (%) <sup>a</sup>	ORAC <sup>b</sup>	Nrf2 Induction Potencies CD (μM) <sup>c</sup>	CatS K <sub>i</sub> (μM) <sup>d</sup>
4a	H	H	H	12	0.86 ± 0.05	n.d. <sup>e</sup>	n.i. <sup>f</sup>
4b	H	NO <sub>2</sub>	H	n.i.	1.36 ± 0.16	82.8 ± 8.4	n.i.
4c	H	H	NO <sub>2</sub>	3	1.54 ± 0.15	n.d.	n.i.
4d	H	=N-O-N=	H	10	1.23 ± 0.23	n.d.	n.i.
4e	H	Cl	H	n.i.	1.15 ± 0.02	n.d.	n.i.
4f	H	OCH <sub>3</sub>	H	19	1.34 ± 0.20	n.d.	n.i.
4g	H	Br	H	n.i.	1.43 ± 0.03	n.d.	n.i.
4h	H	H	Br	7	1.28 ± 0.05	n.d.	55.3 ± 7.4
4i	CH <sub>3</sub>	Cl	H	11	1.93 ± 0.08	96.0 ± 6.1	69.3 ± 5.2
4j	CH <sub>3</sub>	Cl	Cl	12	1.82 ± 0.05	77.2 ± 7.1	n.i.
4k	CH <sub>3</sub>	OCH <sub>3</sub>	H	14	n.i.	69.4 ± 9.1	n.i.
4l	CH <sub>3</sub>	H	OCH <sub>3</sub>	15	0.96 ± 0.07	81.7 ± 11.6	n.i.
nimodipine				37	n.d.	n.d.	n.d.
melatonin				n.d.	2.45 ± 0.09	66.4 ± 16.4	n.d.

<sup>a</sup> Compounds were tested at a concentration of 10 μM. <sup>b</sup> Data are expressed as Trolox equivalents and are the mean (n = 3) ± SEM of two different measurements. <sup>c</sup> Nrf2 induction potencies of test compounds in Nrf2/ARE-luciferase reporter cells. <sup>d</sup> K<sub>i</sub> (± SEM) values were determined in cases of a residual activity ≤ 60% at 50 μM inhibitor concentration. Measurements were done in duplicates with five different inhibitor concentrations as well as in the absence of inhibitor. <sup>e</sup> n.d., not determined, indicates that no experiments were performed. <sup>f</sup> n.i., no inhibition, refers to a residual activity ≥ 95% at 50 μM inhibitor concentration.

**Antioxidant assay.** The antioxidant assessment was conducted by evaluating the compounds 4a–l through the determination of oxygen radical absorbance capacity (ORAC) using the ORAC-Fluorescein (ORAC-FL) method [43] (Table 1). The compounds' radical scavenging properties were quantified in Trolox equivalents (TE), using melatonin as a positive control, which exhibited an ORAC value equal to 2.45 [44]. All compounds except 4k showed antioxidant capacity ranging from 0.86 for 4a to 1.93 for 4i. The best-performing compounds, in descending order, were 4i (1.93 TE), 4j (1.82 TE), and 4c (1.54 TE), being, on



average, only 1.3 times less active than melatonin. From a structure–activity relationship point of view, the absence of a substituent on the aromatic ring was unfavorable for antioxidant activity. The introduction of electron-withdrawing halogen or nitro groups seems to improve this activity, both for compounds with secondary amide groups ( $R^1 = H$ ; e.g., **4c**) and tertiary amide groups ( $R^1 = CH_3$ , e.g., **4i** and **4j**).

**Nrf2 transcriptional activation potencies of compounds 4a–l.** The Nrf2-ARE activating potential of compounds **4a–l** was assessed in vitro by a cell-based luciferase assay using the AREc32 cell line, a reliable cell model for the redox-dependent activation of Nrf2 [45], with melatonin used as a positive control. AREc32 cells were exposed to escalating concentrations of each compound (1, 5, 10, 25, 50, 100, 125, and 150  $\mu M$ ) for 24 h to reach the cytotoxic threshold, followed by measurements of luciferase activity. Melatonin was used as a positive control.

In preliminary assessments, the cytotoxicity of the compounds against AREc32 cells was investigated, showing no toxicity of the compounds up to 100  $\mu M$ . Interestingly, five compounds (**4b**, **4i–l**) exhibited no cytotoxicity up to 150  $\mu M$ , allowing for an investigation of their potential to activate the Nrf2 pathway at this highest concentration. Figures 2 and 3 illustrate that all compounds appear to induce activation of the Nrf2 pathway. However, no significant activity was seen for compounds **4a**, **4c–h**. In contrast, **4b** and **4i–l** caused a significant induction at concentrations up to 150  $\mu M$ . In addition, CD values (i.e., the concentration required to double the specific activity of the luciferase reporter) were calculated for these five compounds to assess their relative potencies. As depicted in Table 1, **4b** and **4i–l** exhibited CD values of 82.2, 96.0, 77.2, 69.4, and 81.7  $\mu M$ , respectively, compared to melatonin's value of 66.4  $\mu M$ . Notably, **4k** showed comparable activity to melatonin, while **4b**, **4i**, **4j**, and **4l** were only 1.2 to 1.5 times less active than melatonin, which represents a recognized Nrf2 activator capable of inducing transcriptional pathways through various mechanisms [46].

Considering the structure–activity relationship, all compounds with a tertiary amide group ( $R^1 = CH_3$ ) possessed the ability to induce the Nrf2 pathway, with the *ortho*-chloro substitution pattern in **4i** being the most advantageous. Among the primary amide derivatives ( $R^1 = H$ ), only the *ortho*-nitro derivative **4b** was active.

**Cathepsins inhibition.** Compounds **4a–l** were then evaluated for their ability to inhibit Cat S. Besides Cat S, the set of assays included three related human cathepsins, B, L, and K, all members of the class of lysosomal cysteine proteases (see Table S1 in the Supporting Information). Following reported procedures, [39–41] percentage or residual activities were determined using chromogenic or fluorogenic peptide substrates, with endpoints measured after 60 min of substrate consumption. To determine  $K_i$  values, progress curves were followed over 60 min and analyzed by linear regression.  $K_i$  values were then obtained by non-linear regression. Two selective inhibitors of cathepsin S were identified, i.e., **4h** and **4i**, showing  $K_i$  values in the two-digit-micromolar range, 55.3 and 69.3  $\mu M$ , respectively, see Table 1. Again, no structure–activity relationship could be established from these results. However, when all the results are considered, it is clear that the tertiary amide compounds appear to be more active against all targets than the secondary analogues.

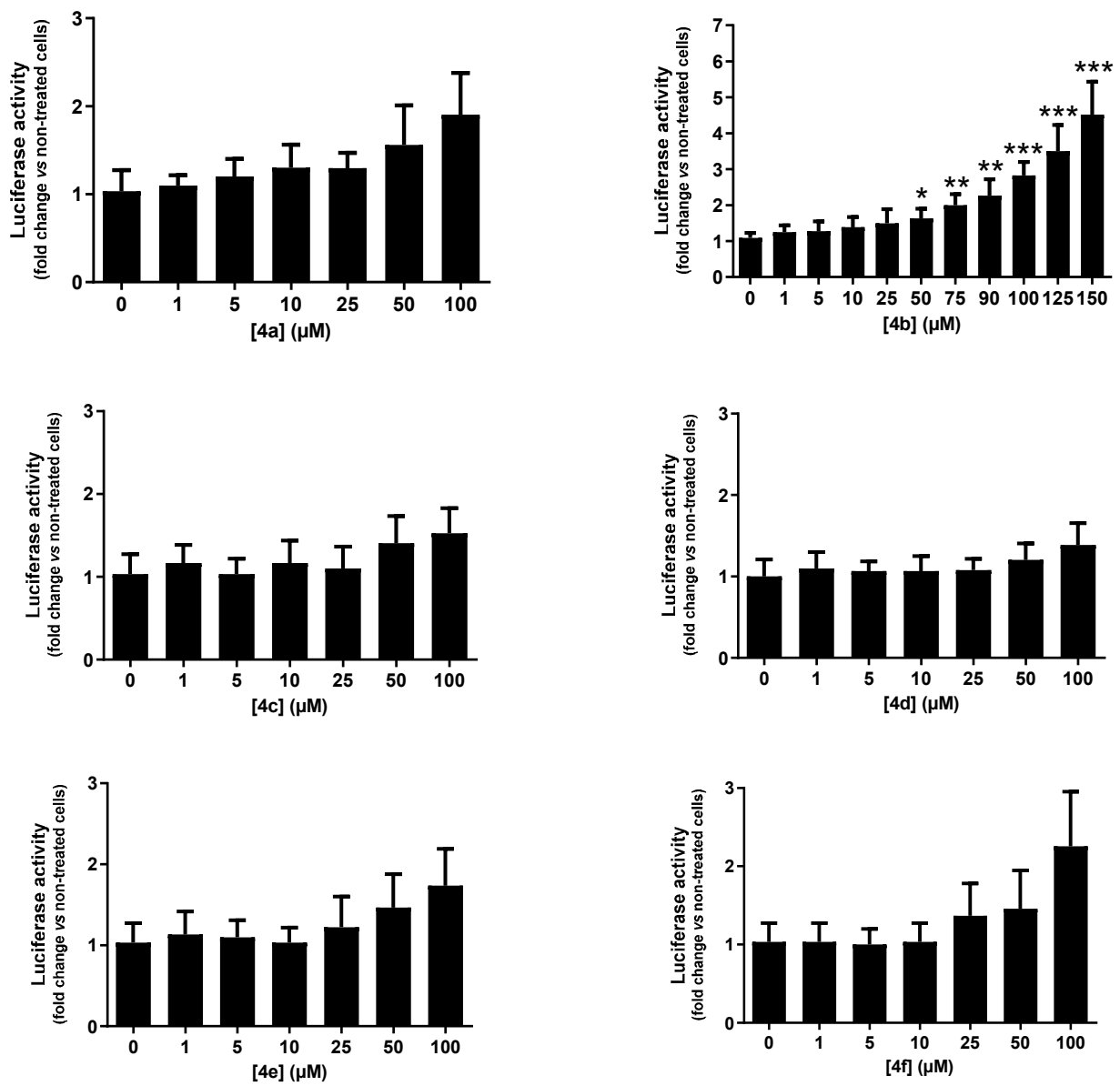


**Figure 2.** Nrf2 transcriptional activation potencies of compounds 4a–f. Data are means  $\pm$  SEM of at least 3 different experiments. \*  $p \leq 0.05$ , \*\*  $p \leq 0.01$  and \*\*\*  $p \leq 0.001$  with respect to non-treated cells (control cells).

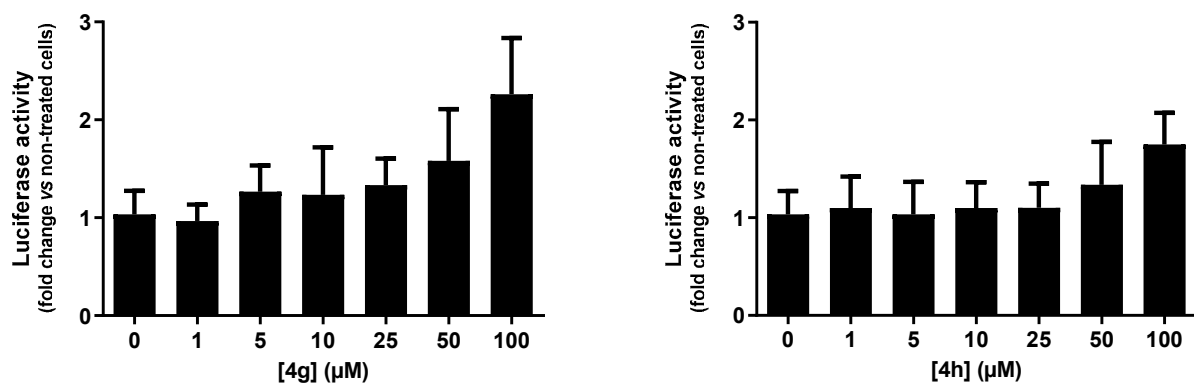


**Figure 3.** Cont.

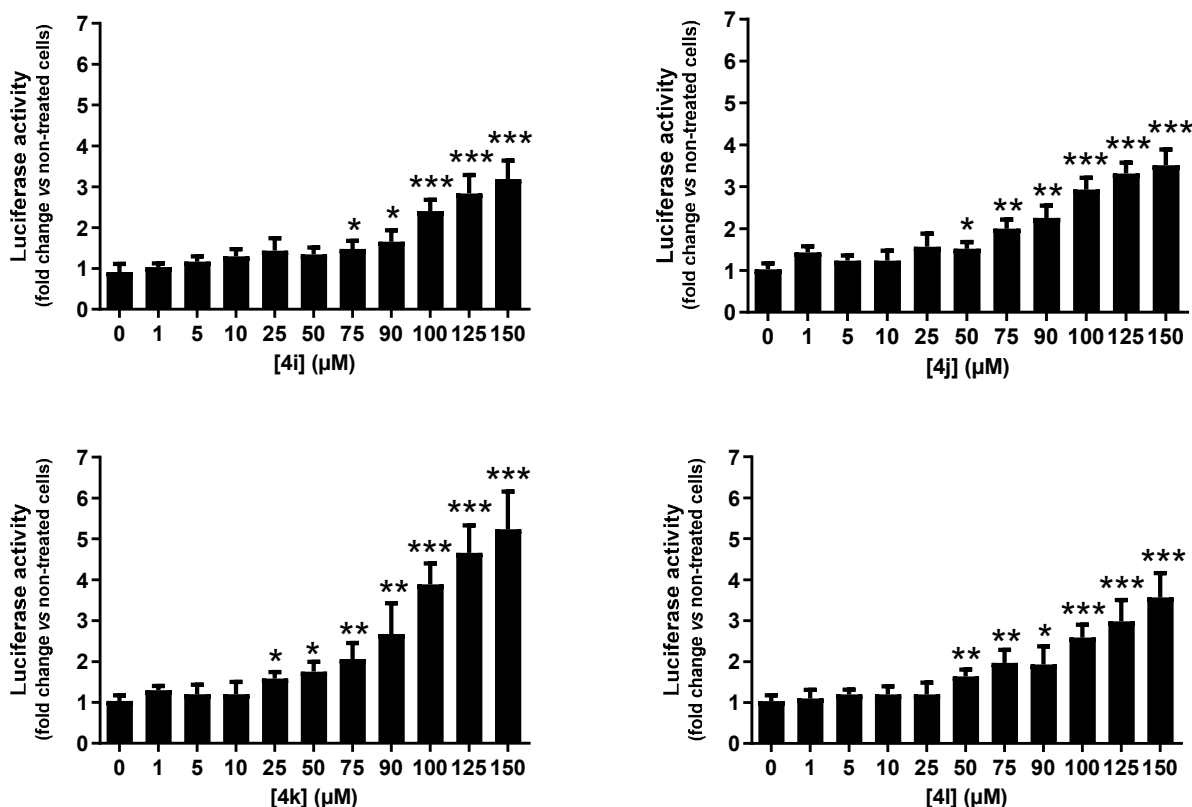


**Figure 3.** Nrf2 transcriptional activation potencies of compounds 4g–l. Data are means  $\pm$  SEM of at least 3 different experiments. \*  $p \leq 0.05$ , \*\*  $p \leq 0.01$  and \*\*\*  $p \leq 0.001$  with respect to non-treated cells (control cells).

#### 4. Conclusions

In this study, we synthesized 12 new compounds via the multi-component Hantzsch reaction, targeting calcium channel inhibition, a strategy whose importance is well established. The design of the compounds was based on the combination of DHPs with propargylamide residues as electrophilic substructures, which proved to be robust and effective. In fact, most of the compounds showed antagonistic activity on calcium channels due to the presence of the DHP scaffold. In addition, almost all the compounds showed antioxidant properties and activated the endogenous Nrf2 antioxidant pathways thanks to the propargylamide moiety. It's noteworthy that only two compounds were identified as inhibitors of cathepsin S, although propargylamides are known to be studied as irreversible inhibitors of cysteine proteases.

In our biological studies, we identified a promising compound, 4i, which showed potent antioxidant activity and the ability to activate Nrf2-ARE pathways. In addition, this compound showed a weak inhibitory effect on Cat S and a modest blockade of calcium channels, three times less active than the reference nimodipine.

This study introduced the first generation of MTDLs combining these biological activities and identified 4i as a promising compound for further research into the treatment of Alzheimer's disease. Ongoing efforts in our laboratories are aimed at developing analogs with the best pharmacological profile and results will be communicated in due course.

**Supplementary Materials:** The following supporting information can be downloaded at <https://www.mdpi.com/article/10.3390/pharmaceutics16010121/s1>, Table S1: Percentage residual activities of human cathepsins in the presence of inhibitors 4a–l @ 50  $\mu$ M, Experimental procedure of ORAC test, Experimental procedure of Nrf2 test and NMR Spectras of compounds 4a–l.

**Author Contributions:** I.P.-A. carried out the synthesis of the molecules. P.J.B., A.S., M.M., A.N. and C.L. performed the biological study. K.J., H.M., M.G. and M.-J.O.-G. supervised the biological assays and edited the manuscript. J.-M.C. and L.L., supervised the project wrote and edited the manuscript the manuscript. All authors have read and agreed to the published version of the manuscript.

**Funding:** This work was supported by the Regional Council of Franche-Comté (2022Y-13659 and 13660 ACCURATE PROJECT).

**Institutional Review Board Statement:** Not applicable.

**Informed Consent Statement:** The data presented in this study are available in Supplementary Material.

**Data Availability Statement:** Samples of the compounds are available from the authors.

**Conflicts of Interest:** The authors declare no conflict of interest.

## References

1. Querfurth, H.W.; LaFerla, F.M. Alzheimer's Disease. *N. Engl. J. Med.* **2010**, *362*, 329–344. [[CrossRef](#)] [[PubMed](#)]
2. Dementia. Available online: <https://www.who.int/news-room/fact-sheets/detail/dementia> (accessed on 11 April 2022).
3. Cacabelos, R. Have There Been Improvements in Alzheimer's Disease Drug Discovery over the Past 5 Years? *Expert Opin. Drug Discov.* **2018**, *13*, 523–538. [[CrossRef](#)] [[PubMed](#)]
4. Bartus, R.T.; Dean, R.L.; Beer, B.; Lippa, A.S. The Cholinergic Hypothesis of Geriatric Memory Dysfunction. *Science* **1982**, *217*, 408–414. [[CrossRef](#)]
5. Gómez-Isla, T.; Hollister, R.; West, H.; Mui, S.; Growdon, J.H.; Petersen, R.C.; Parisi, J.E.; Hyman, B.T. Neuronal Loss Correlates with but Exceeds Neurofibrillary Tangles in Alzheimer's Disease. *Ann. Neurol.* **1997**, *41*, 17–24. [[CrossRef](#)]
6. Chen, C.-H.; Zhou, W.; Liu, S.; Deng, Y.; Cai, F.; Tone, M.; Tone, Y.; Tong, Y.; Song, W. Increased NF- $\kappa$ B Signalling up-Regulates BACE1 Expression and Its Therapeutic Potential in Alzheimer's Disease. *Int. J. Neuropsychopharmacol.* **2012**, *15*, 77–90. [[CrossRef](#)]
7. Oulès, B.; Del Prete, D.; Greco, B.; Zhang, X.; Lauritzen, I.; Sevalle, J.; Moreno, S.; Paterlini-Bréchet, P.; Trebak, M.; Checler, F.; et al. Ryanodine Receptor Blockade Reduces Amyloid- $\beta$  Load and Memory Impairments in Tg2576 Mouse Model of Alzheimer Disease. *J. Neurosci.* **2012**, *32*, 11820–11834. [[CrossRef](#)] [[PubMed](#)]
8. Avila, J.; Pérez, M.; Lim, F.; Gómez-Ramos, A.; Hernández, F.; Lucas, J.J. Tau in Neurodegenerative Diseases: Tau Phosphorylation and Assembly. *Neurotox Res.* **2004**, *6*, 477–482. [[CrossRef](#)]
9. Lemere, C.A.; Munger, J.S.; Shi, G.P.; Natkin, L.; Haass, C.; Chapman, H.A.; Selkoe, D.J. The Lysosomal Cysteine Protease, Cathepsin S, Is Increased in Alzheimer's Disease and Down Syndrome Brain. An Immunocytochemical Study. *Am. J. Pathol.* **1995**, *146*, 848–860.
10. Lowry, J.R.; Klegeris, A. Emerging Roles of Microglial Cathepsins in Neurodegenerative Disease. *Brain Res. Bull.* **2018**, *139*, 144–156. [[CrossRef](#)]
11. Nübling, G.; Schubert, M.; Feldmer, K.; Giese, A.; Holdt, L.M.; Teupser, D.; Lorenzl, S. Cathepsin S Increases Tau Oligomer Formation through Limited Cleavage, but Only IL-6, Not Cathepsin S Serum Levels Correlate with Disease Severity in the Neurodegenerative Tauopathy Progressive Supranuclear Palsy. *Exp. Brain Res.* **2017**, *235*, 2407–2412. [[CrossRef](#)]
12. Yan, M.H.; Wang, X.; Zhu, X. Mitochondrial Defects and Oxidative Stress in Alzheimer Disease and Parkinson Disease. *Free Radic. Biol. Med.* **2013**, *62*, 90–101. [[CrossRef](#)] [[PubMed](#)]
13. Greenough, M.A.; Camakaris, J.; Bush, A.I. Metal Dyshomeostasis and Oxidative Stress in Alzheimer's Disease. *Neurochem. Int.* **2013**, *62*, 540–555. [[CrossRef](#)]
14. Candore, G.; Bulati, M.; Caruso, C.; Castiglia, L.; Colonna-Romano, G.; Di Bona, D.; Duro, G.; Lio, D.; Matranga, D.; Pellicanò, M.; et al. Inflammation, Cytokines, Immune Response, Apolipoprotein E, Cholesterol, and Oxidative Stress in Alzheimer Disease: Therapeutic Implications. *Rejuvenation Res.* **2010**, *13*, 301–313. [[CrossRef](#)] [[PubMed](#)]
15. Rosini, M.; Simoni, E.; Milelli, A.; Minarini, A.; Melchiorre, C. Oxidative Stress in Alzheimer's Disease: Are We Connecting the Dots? *J. Med. Chem.* **2014**, *57*, 2821–2831. [[CrossRef](#)] [[PubMed](#)]
16. Vriend, J.; Reiter, R.J. The Keap1-Nrf2-Antioxidant Response Element Pathway: A Review of Its Regulation by Melatonin and the Proteasome. *Mol. Cell. Endocrinol.* **2015**, *401*, 213–220. [[CrossRef](#)] [[PubMed](#)]
17. Albertini, C.; Salerno, A.; Pinheiro, P.d.S.M.; Bolognesi, M.L. From Combinations to Multitarget-Directed Ligands: A Continuum in Alzheimer's Disease Polypharmacology. *Med. Res. Rev.* **2021**, *41*, 2606–2633. [[CrossRef](#)]
18. Prati, F.; Cavalli, A.; Bolognesi, M.L. Navigating the Chemical Space of Multitarget-Directed Ligands: From Hybrids to Fragments in Alzheimer's Disease. *Molecules* **2016**, *21*, 466. [[CrossRef](#)]
19. Guzior, N.; Wieckowska, A.; Panek, D.; Malawska, B. Recent Development of Multifunctional Agents as Potential Drug Candidates for the Treatment of Alzheimer's Disease. *Curr. Med. Chem.* **2014**, *22*, 373–404. [[CrossRef](#)]
20. Codony, S.; Pont, C.; Griñán-Ferré, C.; Di Pedre-Mattatelli, A.; Calvó-Tusell, C.; Feixas, F.; Osuna, S.; Jarné-Ferrer, J.; Naldi, M.; Bartolini, M.; et al. Discovery and In Vivo Proof of Concept of a Highly Potent Dual Inhibitor of Soluble Epoxide Hydrolase and Acetylcholinesterase for the Treatment of Alzheimer's Disease. *J. Med. Chem.* **2022**, *65*, 4909–4925. [[CrossRef](#)]

21. Szczepańska, K.; Karcz, T.; Dichiara, M.; Mogilski, S.; Kalinowska-Thuścik, J.; Pilarski, B.; Leniak, A.; Pietruś, W.; Podlewska, S.; Popiołek-Barczyk, K.; et al. Dual Piperidine-Based Histamine H3 and Sigma-1 Receptor Ligands in the Treatment of Nociceptive and Neuropathic Pain. *J. Med. Chem.* **2023**, *66*, 9658–9683. [[CrossRef](#)]
22. Ismaili, L.; Monnin, J.; Etievant, A.; Arribas, R.L.; Viejo, L.; Refouvelet, B.; Soukup, O.; Janockova, J.; Hepnarova, V.; Korabecny, J.; et al. (±)-BIGI-3h: Pentatarget-Directed Ligand Combining Cholinesterase, Monoamine Oxidase, and Glycogen Synthase Kinase 3β Inhibition with Calcium Channel Antagonism and Antiaggregating Properties for Alzheimer's Disease. *ACS Chem. Neurosci.* **2021**, *12*, 1328–1342. [[CrossRef](#)] [[PubMed](#)]
23. Dgachi, Y.; Martin, H.; Malek, R.; Jun, D.; Janockova, J.; Sepsova, V.; Soukup, O.; Iriepa, I.; Moraleda, I.; Maalej, E.; et al. Synthesis and Biological Assessment of KojoTacrines as New Agents for Alzheimer's Disease Therapy. *J. Enzyme. Inhib. Med. Chem.* **2019**, *34*, 163–170. [[CrossRef](#)]
24. Malek, R.; Arribas, R.L.; Palomino-Antolin, A.; Totoson, P.; Demougeot, C.; Kobrlova, T.; Soukup, O.; Iriepa, I.; Moraleda, I.; Diez-Iriepa, D.; et al. New Dual Small Molecules for Alzheimer's Disease Therapy Combining Histamine H3 Receptor (H3R) Antagonism and Calcium Channels Blockade with Additional Cholinesterase Inhibition. *J. Med. Chem.* **2019**, *62*, 11416–11422. [[CrossRef](#)]
25. Matos, L.H.S.; Masson, F.T.; Simeoni, L.A.; Homem-de-Mello, M. Biological Activity of Dihydropyrimidinone (DHPM) Derivatives: A Systematic Review. *Eur. J. Med. Chem.* **2018**, *143*, 1779–1789. [[CrossRef](#)]
26. Kang, S.; Cooper, G.; Dunne, S.F.; Luan, C.-H.; James Surmeier, D.; Silverman, R.B. Antagonism of L-Type Ca<sup>2+</sup> Channels Ca<sub>v</sub>1.3 and Ca<sub>v</sub>1.2 by 1,4-Dihydropyrimidines and 4H-Pyrans as Dihydropyridine Mimics. *Bioorg. Med. Chem.* **2013**, *21*, 4365–4373. [[CrossRef](#)] [[PubMed](#)]
27. Cho, H.J.; Jin, S.M.; Youn, H.D.; Huh, K.; Mook-Jung, I. Disrupted Intracellular Calcium Regulates BACE1 Gene Expression via Nuclear Factor of Activated T Cells 1 (NFAT 1) Signaling. *Aging Cell.* **2008**, *7*, 137–147. [[CrossRef](#)]
28. Hayley, M.; Perspicace, S.; Schulthess, T.; Seelig, J. Calcium Enhances the Proteolytic Activity of BACE1: An in Vitro Biophysical and Biochemical Characterization of the BACE1-Calcium Interaction. *Biochim. Biophys. Acta* **2009**, *1788*, 1933–1938. [[CrossRef](#)] [[PubMed](#)]
29. Small, D.H.; Gasperini, R.; Vincent, A.J.; Hung, A.C.; Foa, L. The Role of Aβ-Induced Calcium Dysregulation in the Pathogenesis of Alzheimer's Disease. *J. Alzheimers Dis.* **2009**, *16*, 225–233. [[CrossRef](#)]
30. Anekonda, T.S.; Quinn, J.F. Calcium Channel Blocking as a Therapeutic Strategy for Alzheimer's Disease: The Case for Isradipine. *Biochim. Biophys. Acta* **2011**, *1812*, 1584–1590. [[CrossRef](#)]
31. Irer, S.V.; Alper, G.E.; Sezer, E.D.; Duman, E.; Saatcioglu, F.; Yilmaz, C. The Effect of L-Deprenyl on Tissue mRNA Expressions of NOS Isoforms and NO Levels in an Experimental Diabetes Mellitus Model. *J. Neural Transm.* **2007**, *114*, 811. [[CrossRef](#)]
32. Czerniczyniec, A.; Bustamante, J.; Loeres-Arnaiz, S. Modulation of Brain Mitochondrial Function by Deprenyl. *Neurochem. Int.* **2006**, *48*, 235–241. [[CrossRef](#)]
33. Naoi, M.; Maruyama, W.; Shamoto-Nagai, M. Neuroprotective Function of Rasagiline and Selegiline, Inhibitors of Type B Monoamine Oxidase, and Role of Monoamine Oxidases in Synucleinopathies. *Int. J. Mol. Sci.* **2022**, *23*, 11059. [[CrossRef](#)]
34. Nakaso, K.; Nakamura, C.; Sato, H.; Imamura, K.; Takeshima, T.; Nakashima, K. Novel Cytoprotective Mechanism of Anti-Parkinsonian Drug Deprenyl: PI3K and Nrf2-Derived Induction of Antioxidative Proteins. *Biochem. Biophys. Res. Commun.* **2006**, *339*, 915–922. [[CrossRef](#)] [[PubMed](#)]
35. Arkona, C.; Rademann, J. Propargyl Amides as Irreversible Inhibitors of Cysteine Proteases—A Lesson on the Biological Reactivity of Alkynes. *Angew. Chem. Int. Ed.* **2013**, *52*, 8210–8212. [[CrossRef](#)]
36. Xu, J.; Wang, H.; Ding, K.; Lu, X.; Li, T.; Wang, J.; Wang, C.; Wang, J. Inhibition of Cathepsin S Produces Neuroprotective Effects after Traumatic Brain Injury in Mice. *Mediat. Inflamm.* **2013**, *2013*, e187873. [[CrossRef](#)] [[PubMed](#)]
37. Clemens, R.J.; Hyatt, J.A. Acetoacetylation with 2,2,6-Trimethyl-4H-1,3-Dioxin-4-One: A Convenient Alternative to Diketene. *J. Org. Chem.* **1985**, *50*, 2431–2435. [[CrossRef](#)]
38. Malek, R.; Simakov, A.; Davis, A.; Maj, M.; Bernard, P.J.; Wnorowski, A.; Martin, H.; Marco-Contelles, J.; Chabchoub, F.; Dallemagne, P.; et al. Biginelli Reaction Synthesis of Novel Multitarget-Directed Ligands with Ca<sup>2+</sup> Channel Blocking Ability, Cholinesterase Inhibition, Antioxidant Capacity, and Nrf2 Activation. *Molecules* **2023**, *28*, 71. [[CrossRef](#)]
39. Frizler, M.; Lohr, F.; Lülsdorff, M.; Gütschow, M. Facing the Gem-Dialkyl Effect in Enzyme Inhibitor Design: Preparation of Homocycloleucine-Based Azadipeptide Nitriles. *Chem. Eur. J.* **2011**, *17*, 11419–11423. [[CrossRef](#)]
40. Lemke, C.; Benýšek, J.; Brajtenbach, D.; Breuer, C.; Jílková, A.; Horn, M.; Buša, M.; Ulrychová, L.; Illies, A.; Kubatzky, K.F.; et al. An Activity-Based Probe for Cathepsin K Imaging with Excellent Potency and Selectivity. *J. Med. Chem.* **2021**, *64*, 13793–13806. [[CrossRef](#)]
41. Mertens, M.D.; Schmitz, J.; Horn, M.; Furtmann, N.; Bajorath, J.; Mareš, M.; Gütschow, M. A Coumarin-Labeled Vinyl Sulfone as Tripeptidomimetic Activity-Based Probe for Cysteine Cathepsins. *Chembiochem* **2014**, *15*, 955–959. [[CrossRef](#)]
42. Tamaddon, F.; Razmi, Z.; Jafari, A.A. Synthesis of 3,4-Dihydropyrimidin-2(1H)-Ones and 1,4-Dihydropyridines Using Ammonium Carbonate in Water. *Tetrahedron Lett.* **2010**, *51*, 1187–1189. [[CrossRef](#)]
43. Dávalos, A.; Gómez-Cordovés, C.; Bartolomé, B. Extending Applicability of the Oxygen Radical Absorbance Capacity (ORAC—Fluorescein) Assay. *J. Agric. Food Chem.* **2004**, *52*, 48–54. [[CrossRef](#)] [[PubMed](#)]
44. Benchekroun, M.; Ismaili, L.; Pudlo, M.; Luzet, V.; Gharbi, T.; Refouvelet, B.; Marco-Contelles, J. Donepezil–Ferulic Acid Hybrids as Anti-Alzheimer Drugs. *Future Med. Chem.* **2015**, *7*, 15–21. [[CrossRef](#)] [[PubMed](#)]



45. Wang, X.J.; Hayes, J.D.; Wolf, C.R. Generation of a Stable Antioxidant Response Element–Driven Reporter Gene Cell Line and Its Use to Show Redox-Dependent Activation of Nrf2 by Cancer Chemotherapeutic Agents. *Cancer Res.* **2006**, *66*, 10983–10994. [[CrossRef](#)]
46. Parada, E.; Buendia, I.; León, R.; Negredo, P.; Romero, A.; Cuadrado, A.; López, M.G.; Egea, J. Neuroprotective Effect of Melatonin against Ischemia Is Partially Mediated by Alpha-7 Nicotinic Receptor Modulation and HO-1 Overexpression. *J. Pineal Res.* **2014**, *56*, 204–212. [[CrossRef](#)]

**Disclaimer/Publisher’s Note:** The statements, opinions and data contained in all publications are solely those of the individual author(s) and contributor(s) and not of MDPI and/or the editor(s). MDPI and/or the editor(s) disclaim responsibility for any injury to people or property resulting from any ideas, methods, instructions or products referred to in the content.